TIMING WINDOW AND OPTIMIZATION FOR POSITION RESOLUTION AND ENERGY CALIBRATION OF SCINTILLATION DETECTOR

J. Zhu, M.H. Fang, J. Wang, Z.Y. Wei§
Nanjing University of Aeronautics and Astronautics, Nanjing 210016, P. R. China

Abstract

We studied fast plastic scintillation detector array. The array consists of four cuboid bars of EJ200， each bar with PMT readout at both ends. The geometry of the detector, energy deposition in the scintillator， signal generation and energy response have been simulated based on Monte Carlo. The detection efficiency and the real events selection have been obtained while the background noise has been reduced by using two-end readout timing window coincidence. We developed an off-line analysis code, which is suitable for massive data from the digitizer. We set different coincidence timing windows, and did the off-line data processing respectively. It can be shown that the detection efficiency increases as the width of the timing window increases, and when the width of timing window is more than 10 ns, the detection efficiency will slowly grow until it reaches saturation. Therefore, the best timing window parameter τ as 16 ns is obtained for the on-line coincidence measurement. When exposure to ^{137}Cs γ -ray irradiation, a 12 cm position resolution can be achieved while reaching the timing resolution of 0.9 ns. The pulse integration of signals of the detector is in proportion to the energy of incident particles. Furthermore, the geometrical mean of the dual-ended signals, which is almost independent of the hit position, could be used as the particle energy. Therefore, this geometrical mean as the energy of incident particle is calibrated via the Compton edges of ^{60}Co source, ^{137}Cs source and the natural ^{40}K, ^{208}Tl, and the reliability of the calibration results has been improved. Besides, the energy response is linear.

INTRODUCTION

When an incident particle interacts in a scintillator, it can cause ionization and excitation of the atoms and molecules of the scintillator. The energy of the incident particle is deposited in the scintillator [1]. The decay of excited atoms and molecules back to their ground states results in a emission of photons with two decay components: the fast one with decay time less than a nanosecond， and the slow one has decay time of hundreds of nanoseconds. The photons are collected on photocathode of the photomultiplier tube (PMT), and then these photons are converted to photoelectrons and amplified. The output signals of the scintillation detector depend on both the energy and the hit position of the incident particle. Besides, false signals come from the dark current and noise also. When the dual-ended readout is taken, we need methods to get hit position and energy of the particles, and also need to select the real events [2]. In this paper, we got real events from incident particles with the background noise reduced by using two-end readout timing window coincidence.

EJ-200 plastic scintillation detector array and its data acquisition system have been set up for radiation measurement in our laboratory. The scintillation detector array consists of four EJ-200 plastic scintillators which have dual-ended PMTs. The EJ-200 plastic scintillator combines two main benefits of long optical attenuation length and fast timing. On the basis of coincidence measurement, we picked out the real events from the timing window of signals, and optimized the timing resolution, position resolution and energy response of the detector.

SCINTILLATION DETECTION AND DATA ACQUISITION SYSTEM

The plastic scintillator used in this work was provided by the ELJEN Enterprises, USA. The scintillator (denoted by the ELJEN number EJ-200) had dimensions: 5 cm × 5 cm × 125 cm. The decay time of the scintillator is at the level of ns, and the rise time is less than 1 ns. The EJ-200 plastic scintillator was coupled to an ET Enterprises 9813B PMT. A VME bus system was used in our laboratory, and a schematic diagram of the detection system is shown in Fig. 1.

The DT5751 is a 4 channels 10 bit 1 GS/s Desktop Waveform Digitizer with 1 Vpp input dynamic range on single ended MCX coaxial connectors. The DT5751 Waveform Digitizer, which is taken in on-line coincidence measurement, has replaced some complex modules in the traditional coincidence circuits.

The V6533 is a 6 channels High Voltage Power Supply in 1 unit wide VME 6U module.

The online Digital Pulse Processing for Pulse Shape Discrimination firmware (DPP-PSD) was used in this study. Under the frame of DPP-PSD, we got the on-line waveforms and the energy histograms. Besides, the lists for the on-line data were obtained from the digitizer, and were further processed by ROOT, an off-line data-analysis software.

§ email address: wzy_msc@nuaa.edu.cn

ISBN 978-3-95450-177-9

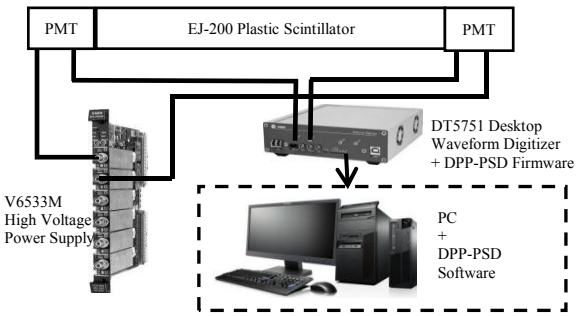

Figure 1: Schematic diagram of the experimental setup.

SIMULATION AND ITS RESULTS

The core idea of the coincidence measurement is to pick out the real event according to the timing window of signals. The key technical parameter of the coincidence circuits is the coincidence timing window τ. See in Fig. 2, if x, the distance between the hit position and the left side of the scintillator, corresponds to time t_1, and L-x, the distance between the hit position and the right side of the scintillator, corresponds to time t_2, then, the timing window of signals can be represented by $\tau = |t_1 - t_2|$. If the incident particles hit in the middle of the detector, $|t_1 - t_2| = 0$; If the incident particles hit in either end of the detector, $|t_1 - t_2|$ is up to the maximum value of the timing window. The true events take place in the span of $|t_1 - t_2|$. When the time interval between two pulses is less than τ, it outputs the coincidence pulse; otherwise it rejects. The timing window parameter can be used both in on-line analysis and off-line analysis.

The detector has been simulated based on Monte Carlo, including its geometry and particle interactions in the scintillator.

In Fig. 2, x, the distance between the hit position and the left side of the scintillator, is shown, and Δt, the time difference between the signals at both ends of the detector, is shown in Fig. 3, then, the $\Delta t - x$ curve is simulated in Fig. 4.

In Fig. 4, the time difference of signals at both ends of the scintillator is linear to the distance x, and $\Delta t - x$ is linear up to 9 ns. Considering the transit-time jitter of the PMT, which is determined as 1.17 ns, then, the maximum time difference in case of a true event is estimated to be 11 ns.

We developed an off-line analysis code, which is suitable for massive data from the digitizer, in order to find a reasonable timing resolution window for on-line experiment. The detection efficiency $\varepsilon_c(t)$ can be expressed as the ratio between the number of the coincidence particles(denoted by N_c) and the number of the particles produced by the radiation source during detection (denoted by N), which as shown in Eq. (1):

$$\varepsilon_c(t) = \frac{N_c}{N} \times 100\% \quad . \qquad (1)$$

The simulations based on the ^{137}Cs γ-ray source were done. The experiment time is 1000 s. Set different coincidence timing windows, and do the off-line data processing respectively. Detection efficiency versus coincidence timing window is given in Fig. 5. The black dots in the figure stand for experiment data and the curve is a fitted curve obtained by the off-line programs based on ROOT. It can be observed that detection efficiency is changing over the value of the coincidence timing window, and the width of timing window is more than 10 ns, the detection efficiency will slowly grow until it reaches about 20%. Therefore, this paper sets the best timing window parameter τ as 16 ns for the on-line coincidence measurement.

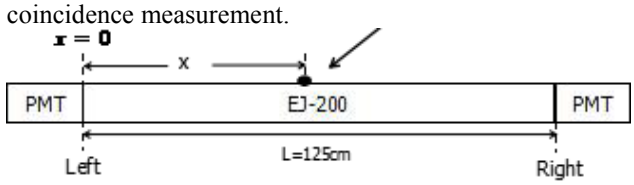

Figure 2: Schematic diagram of the distance between the hit position and the left side of the scintillator.

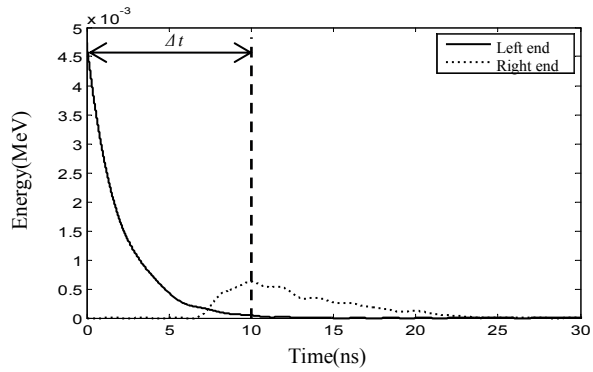

Figure 3: Schematic diagram of the time difference between the signals at both ends of the detector (x=0).

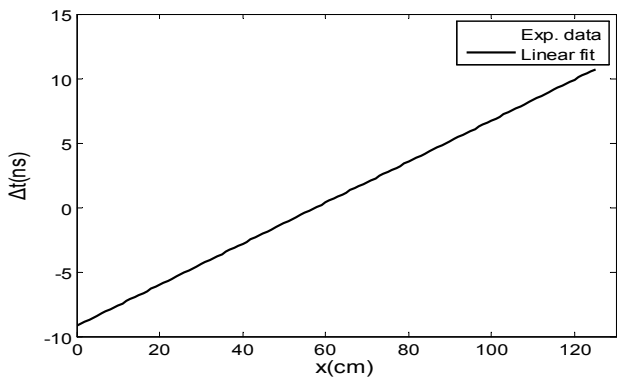

Figure 4: Δt (ns) , time difference of signals at both ends of the detector vs. x (cm), the distance between the hit position and the left side of the scintillator.

POSITION RESOLUTION AND ENERGY RESPONSE

This paper finds the best coincidence timing window parameter as 16 ns for the on-line coincidence measurement, see Fig. 5.

ISBN 978-3-95450-177-9

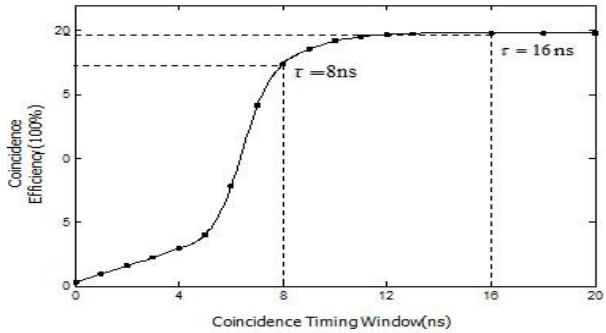

Figure 5: Detection efficiency vs. the coincidence timing window for the scintillation detector.

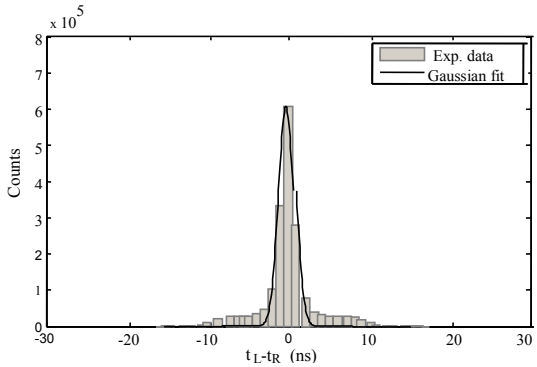

(a) in the middle

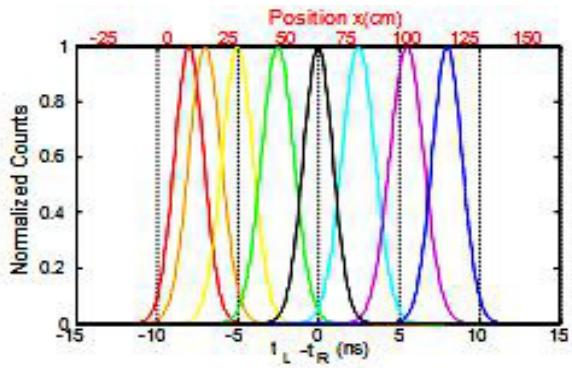

(b) on different positions

Figure 6: Time difference of signals generated from real events at both ends of the scintillator through Gaussian fitting with the ^{137}Cs source (a) in the middle of the scintillator and (b) on different positions.

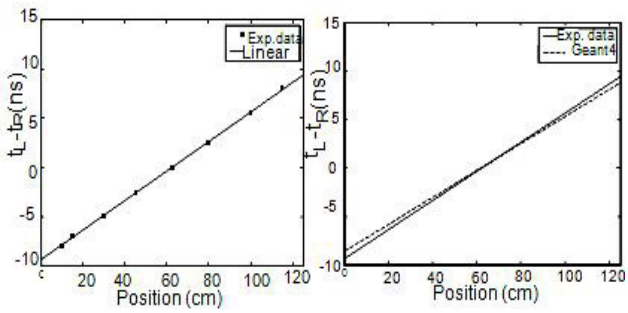

Figure 7: Time difference versus the position of the radiation source : experiment results (left) and simulation results by Geant4 code (right).

Since the two PMTs at both end of the plastic scintillation detector studied in this work are nearly the same, the timing resolution of the detector, σ_t , can be defined as Eq. (2):

$$\sigma_t^2 = \sigma_1^2 + \sigma_2^2 . \quad (2)$$

Where σ_1 and σ_2 represent the timing resolution at each end of the detector, respectively. Besides, if the scintillator used in this work has the intrinsic timing resolution (denoted by σ_s) and substituting the transit-time spread of the PMT, σ_{PMT} , for its timing resolution [3], and then σ_t , the timing resolution of the scintillation detector in this work can be represented by Eq. (3):

$$\sigma_t^2 = \sigma_s^2 + 2\sigma_{PMT}^2 . \quad (3)$$

The effective transmission speed of the signals in the scintillator is represented by c_{eff} [4]. Furthermore, it has been concluded that the integral charge of the signals at both ends, $\ln(Q_L/Q_R)$, is linearly associated with x. Therefore, the position resolution σ_x is shown as Eq. (4):

$$\sigma_x = \sigma_t \times c_{eff} . \quad (4)$$

By exposing the scintillation detector to the ^{137}Cs γ -ray source, a timing resolution of 0.9 ns is reached (when the best coincidence timing window $\tau = 16$ ns), see Fig. 6. Time difference of signals, which is generated from real events at both ends of the scintillator, and the position of the radiation source is near to a linear relationship (see Fig. 7), which fits the simulation results by Geant4. In Fig. 7, the slope of the fit line is 0.15, and the position resolution of the detector reaches 12 cm. The pulse integration of signals of the detector is in proportion to the energy of incident particles [5]. Furthermore, the geometrical mean of the dual-ended signals, which is almost independent of the hit position, could be used as the particle energy (see Eq. (5)):

$$Q_{GM} = \sqrt{Q_L Q_R} . \quad (5)$$

Where Q_{GM} represents the the geometrical mean of the dual-ended signals, and Q_L (or Q_R) represents the integral charge of the signals at the left (or right) end of the detector .

Therefore, this geometrical mean as the energy of incident particle is calibrated via the Compton edges of ^{60}Co source, ^{137}Cs source and the natural ^{40}K, ^{208}Tl, and the reliability of the calibration results has been improved. The gamma ray energy, E_γ, Compton edges, E_0, the ADC number of the photopeak, ch_p, the standard deviation of the photopeak, σ, the ADC number of the Compton edges,

ISBN 978-3-95450-177-9

ch_c, are listed in Table 1. The energy calibration of the detector see Fig. 8. It is shown that the energy response is linear within the lower energy range.

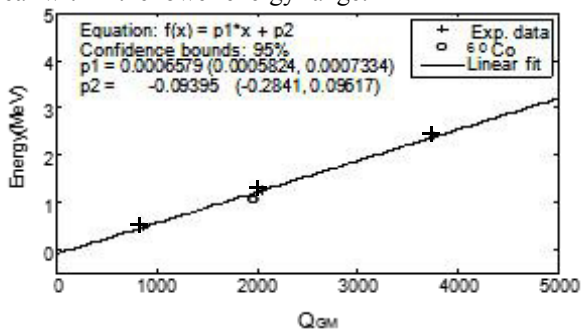

Figure 8: The energy calibration of the detector : crosses are experimental data and the curve represents the best-fitting.

Table 1: The Compton Edges of Different Radioactive Sources

γ	$E_{\gamma(MeV)}$	$E_{0(MeV)}$	ch_p	σ	ch_c
^{60}Co	1.173 1.333	1.0408	1603	312	1968
^{137}Cs	0.662	0.4777	679	154	860
^{40}K	1.461	1.2435	1710	289	2048
^{208}Tl	2.614	2.3812	3148	520	3756

CONCLUSION

The real event selection, timing resolution, position resolution and energy response of the EJ-200 plastic scintillation detector have been analyzed using timing window coincidence measurement. The detector was simulated based on Monte Carlo, including its geometry, energy deposition in the scintillator, photon collection and signal generation. The decay time of the pulse of scintillator is at the level of ns, and the rise time is less than 1 ns. Theoretical derivation and simulation results showed that Δt , time difference of signals at both ends of the detector, was linear with x, distance between the hit position and the left side of the scintillator, and Δt -x curve was linear up to 9 ns. Besides, time and position response have been measured by exposing to a ^{137}Cs γ -ray source. The best coincidence timing window parameter is 16 ns, and the position resolution is up to 12 cm. Since the pulse integration of signals of the detector is in proportion to the energy of incident particles, the geometrical mean of the dual-ended signals, which is almost independent of the hit position, could be used as the particle energy to calibrate the energy response of the detector via the Compton edges of ^{60}Co source, ^{137}Cs source and the natural ^{40}K, ^{208}Tl. The reliability of the calibration results has been improved. It was shown that the energy response of the detector was linear within the experimental energy range.

REFERENCES

[1] A. V. Kuznetsov *et al.*, "Position-sensitive neutron detector", *Nuclear Instruments and Methods in Physics Research A*, vol. 477, pp. 372–377, 2002.

[2] Wu, Zhihua *et al.*, *The research methods of nuclear physics,* Beijing: Atomic Energy Press, 1997.

[3] Liu,Yang *et al.*, "Measurement of TTS of Fine-Mesh PMT with Cherenkov Light", *Journal of University of Science and Technology of China*, vol. 35, no. 5, pp. 608-612, 2005.

[4] L. Lüdemann, K. Knoche *et al.*, "A Large-area Position-sensitive Detector for Fast Neutrons", *Nuclear Instruments and Methods in Physics Research A*, vol. 334, pp. 495-503, 1993.

[5] L. Karsch, A. Bohm *et al.*, "Design and Test of A Large-area Scintillation Detector for Fast Neutrons" , *Nuclear Instruments and Methods in Physics Research A*, vol. 460, pp. 362-367, 2001.

ISBN 978-3-95450-177-9